

Observation of Black-body Radiation and Emission Spectra of Alkali Metals by Using Visible Light Spectroscopy

Haci Berkay Buz^{1,*}

¹*Department of Physics, Bilkent University, Ankara 06800, Türkiye*

(Dated: May 13, 2025)

Black-body radiation and emission spectra of atoms are path-breaking concepts in modern physics which demonstrate quantization of energy. The idea of discontinuous energy later led to quantum theory. In this experiment, it was aimed to verify Planck's distribution law for the black-body radiation and observe the emission spectra of the alkali metal atoms. The intensity and wavelength distribution of black-body radiation of incandescent light bulb was measured and the curve shift towards lower wavelengths was observed. The emission spectrum of the excited atoms were measured with ± 3 nm accuracy. In both parts of the experiment, these groundbreaking discoveries were observed with the visible light spectrometer we have built.

INTRODUCTION

Black-body radiation and atomic emission spectra are two of the fundamental phenomena in physics, providing deep insight into the quantum nature of light and matter. In the late 19th century, classical physics failed to explain the observed distribution of black-body radiation, leading to what became known as the "ultraviolet catastrophe." According to classical theory, the intensity of radiation emitted by a black body should increase indefinitely with decreasing wavelength, which contradicted experimental results. To resolve this, Max Planck introduced the concept of quantized energy, proposing that energy is emitted in discrete units, or "quanta," rather than continuously. This leads to the beginning of quantum theory [1].

The study of atomic spectra began when scientists discovered that dark lines in sunlight matched the bright lines emitted by heated elements. This led to Kirchhoff's law showing that atoms absorb and emit light at the same wavelengths. In the 1950s, researchers developed practical ways to use these spectral lines for chemical analysis. Today, this principle remains fundamental to understanding atomic structure and behavior [2].

The understanding of black-body radiation has since played a key role in numerous technological and scientific developments. In as-

trophysics, it enables the estimation of stellar temperatures and compositions by analyzing the emitted spectrum from stars [3]. Similarly, emission spectra are critical in identifying atomic structures and elements. For example, flame test emission spectra is widely used in identifying metal ions by their characteristic emission lines [2].

In this project, the aim was to experimentally analyze black-body radiation at various temperatures and to observe the discrete emission spectra of alkali metal compounds. A visible-light spectrometer was constructed using a webcam and a compact disc (CD) as a diffraction grating. The black-body spectrum of a tungsten filament bulb was measured at different voltages to observe the effect of temperature on the radiation curve. Then, LiCl, NaCl, KBr compounds were excited using a Bunsen burner to observe the emission lines of lithium, sodium, and potassium atoms.

THEORY

Black Body Radiation

An object emits electromagnetic waves with different wavelengths that vary with its temperature. The scientists adopted the concept of energy density (u) which corresponds to the

energy possessed by electromagnetic waves per unit volume in a given region to explain this phenomenon.

$$du(\lambda, T) = \rho(\lambda, T)d\lambda \quad (1)$$

$\rho(\lambda, T)$ indicates the density of states, and λ and T correspond to the wavelength of the emitted light and the temperature of the object, respectively. For a fixed temperature, the higher $\rho(\lambda, T)$ indicates that the energy is greater between λ and $\lambda + d\lambda$. If the both sides are integrated, total energy density u is obtained as

$$u(T) = \int_0^\infty \rho(\lambda, T)d\lambda \quad (2)$$

which depends on T as expected. The total energy is:

$$E(T) = Vu(T) \quad (3)$$

where V corresponds to the volume of a given region. Here, the German physicist Max Planck introduced the idea of the quantization of energy, which corresponds to the limitation of energy in certain ranges. Eventually, he was able to derive a formula for $\rho(\lambda, T)$, which is called Planck distribution:

$$\rho(\lambda, T) = \frac{8\pi hc}{\lambda^5(e^{\frac{hc}{\lambda kT}} - 1)} \quad (4)$$

where h is Planck's constant and k is the Boltzmann's constant.

In this experiment, an incandescent light bulb was used, with a tungsten filament that can reach temperatures above 2500 K. Planck distribution of an object with 1500K, 2000K and 2500K is given below:

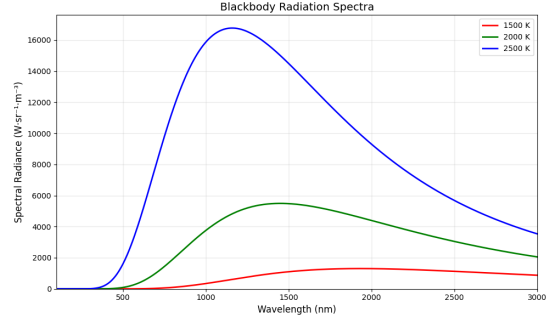


FIG. 1. Planck's Distribution at 1500K, 2000K and 2500K

By Equation 4, this distribution would shift to right for decreasing temperatures. It was aimed to observe this shift by using light spectroscopy [4].

Heat Transfer via Radiation

From Equation 4, total energy density per unit volume can be obtained by integrating along λ as follows:

$$u(T) = \int_0^\infty \frac{8\pi hc}{\lambda^5(e^{\frac{hc}{\lambda kT}} - 1)} d\lambda = \frac{8\pi^5 k^4}{15(hc)^3} T^4 \quad (5)$$

This equation can be written as:

$$u(T) = \sigma \frac{T^4}{c}$$

where $\sigma = \frac{8\pi^5 k^4}{15(hc)^3} = 5.6704 \times 10^{-8} W/m^2 \cdot K^4$. Here, energy flux density which is the rate of energy emission per unit area is defined as:

$$J_u(T) = \frac{cU(T)}{V} = cu(T)$$

If $u(T)$ is put in this equation, it is obtained that:

$$J_u(T) = \sigma T^4$$

This relation is valid for perfect black-bodies. Since tungsten is not a perfect black-body radiator, a emissivity coefficient ε is needed to add.

$$J_u(T) = \sigma \varepsilon T^4$$

So if both sides are multiplied by the area of the blackbody, the total power [5]:

$$P(T) = \sigma \varepsilon A T^4 \quad (6)$$

When the system reaches thermal equilibrium, Equation 6 and power output of the circuit $P_c = I^2 R$ should be equal. Thanks to this equation, it is aimed to find the temperature of the tungsten wire with simple circuit components such as current, resistance, voltage. The light bulb used in this experiment had specifications 24W, 2700K. So constants of the equation can be found and this equation simplifies to

$$T = \left(\frac{V^2}{1.171 \times 10^{-11} \text{ V}^2/\text{K}^4} \right)^{\frac{1}{4}} \quad (7)$$

where V is the voltage applied.

Emission Spectra

The emission spectra of atoms arise from electrons transitioning between quantized energy levels, emitting photons with specific wavelengths. These energy levels can be calculated by solving the time-independent Schrodinger equation:

$$\left[-\frac{\hbar^2}{2m} \nabla^2 + V(\vec{r}) \right] \psi(\vec{r}) = E\psi(\vec{r}) \quad (8)$$

where the first term represents the kinetic energy and $V(\vec{r})$ is the potential energy of the electron. For hydrogen-like atoms (with one electron), this equation can be solved analytically. However, for multi-electron atoms such as lithium, sodium, and potassium, the situation becomes much more complex. This is due to electron-electron interactions, which make the

system a many-body problem with no exact analytical solution. Instead, it must be approximated using perturbation methods or numerical techniques, which involve advanced mathematics and are beyond the scope of this course.

Because of this difficulty, the spectral lines of such atoms are usually obtained from reliable spectroscopic databases rather than direct calculation. In this study, the observed emission lines of Li, Na, K, and Sr were compared to the tabulated values from standard reference materials [6].

Diffraction Grating

Diffraction grating creates a phase difference by diffraction of light and creates constructive and destructive interference owing to this phase difference. Since the angle of diffraction depends on the wavelength of light, wavelengths can be determined by looking at the position where the light falls. There are two types of diffraction grating. One of them is transmission phase grating, where light passes through the grating and diffracts, and the other is reflection phase grating, where light is reflected from the surface of the grating. In this experiment, reflection grating was used. The equation for the reflection grating is:

$$d \cdot (\sin \theta_m - \sin \theta_i) = m\lambda \quad (9)$$

where d is spacing between grooves, m is diffraction order, θ_m is the m th order diffraction angle, θ_i is the incidence angle and λ is the wavelength of the light. Equation shows that λ cannot be bigger than d . In the specifications of the CD used, it is seen that the groove spacing corresponds to the track pitch and this is 1510 nm. The grooves progress in a spiral shape starting from the middle of the CD [7].

METHODOLOGY

The experimental setup consists of a slit (made from 2 vertical razor blades) to control the amount of incoming light, a CD acting as a diffraction grating, a light diffuser to ensure homogeneous light distribution, and a 2K webcam to capture and analyze the diffracted light (see FIG 2).



FIG. 2. Final version of the experimental setup.

1. A digital camera was initially selected for the experiment because it was expected to provide higher-quality images. However, it did not allow real-time image processing and could not focus at short distances. Therefore, it was replaced with a webcam. To extend the detection range beyond the visible spectrum, the infrared filter on the webcam was removed. This enabled us to collect data up to approximately 950 nm, based on the obtained spectrum.
2. A DVD was initially used as the diffraction grating. It gave reasonable results but was not effective at measuring near-infrared wavelengths because of its small groove spacing (about 740 nm). CDs have a larger groove spacing of around 1500 nm. This allows them to diffract longer wavelengths, as explained in Equation 9 [7]. For this reason, a CD was chosen instead of a DVD to also get infrared spectrum. By adjusting the CD and webcam angle optimal results were achieved.
3. Since the grooves on a CD form a spiral pattern rather than straight lines, the center of the CD was aligned with the camera. This ensures that the diffraction pattern was a straight line. Misalignment would have resulted in angled spectra that affects the accuracy of the measurements. Three diffraction beams were observable when CD was used. The webcam was positioned to capture the brightest of these beams for optimal data collection.
4. The data captured by the webcam was processed using the software Theremino Spectrometer. Initially, it was observed that the shape of the spectrum varied depending on the position of the light source. To address this, the wall around the slit was thickened to ensure that the incoming light followed a straight path. Additionally, a light diffuser was used to distribute the incoming light uniformly. In the end, a stable and consistent spectrum was obtained.
5. During the calibration of the spectrometer, the slit width was adjusted based on the intensity of the light source. A wider slit was used for the flame color test to increase light intensity, while a narrower slit was employed for the blackbody spectrum to enhance resolution. Calibration was performed using green (532 ± 10 nm) and red (655 ± 10 nm) laser pointers. Although the ± 10 nm uncertainty is relatively large, it was considered acceptable. Because the laser wavelengths showed agreement within ± 2 nm when compared with known spectral peaks from a phone screen (blue: 463 nm, green: 523 nm, red: 610 nm) [8]. Calibration was completed by shining the laser onto the grating and matching the measured positions with the known laser wavelengths on the software.
6. In the first stage of the experiment, the blackbody spectrum at different temperatures was recorded by varying the voltage

applied to the light source. A 25V, 24W incandescent bulb with a color temperature of 2700K was used for this purpose. The constants in Equation 6 were determined using the known color temperature of the 24W bulb. Subsequently, temperatures at different voltages were calculated using Equation 7. The theoretical blackbody distributions were plotted and compared with the experimentally obtained spectra.

7. In the second stage of the experiment, LiCl, NaCl, and KBr compounds were excited using a Bunsen burner to observe the emission spectra of Li, Na, and K atoms. Due to the poor sensitivity of the spectrometer to low-intensity light, only the brightest emission lines were detectable. The observed spectral data were then compared with data table.

RESULTS

Blackbody Radiation

Imperfections in the CD and camera limitations prevented a smooth blackbody spectrum. However, this does not hinder comparative analysis. As shown in FIG. 3, the spectrum within the 450–600 nm range closely follows theoretical expectations. In contrast, significant deviations occur beyond this range. Therefore, only the 450–600 nm region will be used in subsequent analyses.

Temperature values corresponding to different applied voltages were calculated using Equation 7. The theoretical blackbody curves were adjusted to match the experimental data at 450 nm, where the spectrometer started giving consistent results. Then, both the curve shapes and the relative intensities were compared across different measurements.

The first dataset corresponds to 10V, yielding an approximate temperature of 1771 K (see FIG. 4). While some local deviations

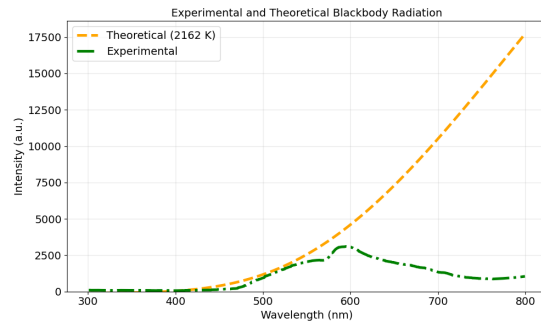


FIG. 3. Comparison of theoretical and experimental spectra for 16V (2162K). Data beyond 600 nm shows significant deviation and is therefore excluded from the analysis. “a.u.” stands for arbitrary units.

are present, the overall shape of the experimental curve shows good agreement with the theoretical blackbody distribution. However, between 450–520 nm, the experimental curve is flatter than expected. This may be due to the spectrometer’s limited sensitivity, which made it difficult to detect low intensity values. At 14V (2022 K), the experimental curve

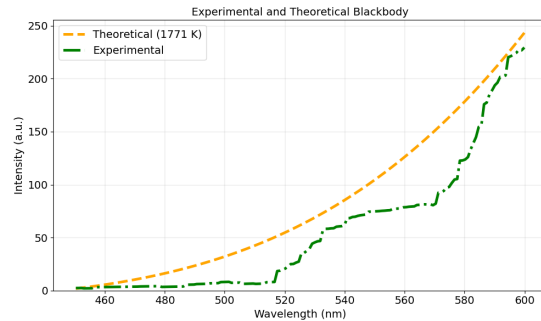


FIG. 4. Comparison of the 10V experimental spectrum and the corresponding 1771K blackbody distribution. Noticeable deviations from theory occur in the 450–520 nm and 550–580 nm intervals. “a.u.” stands for arbitrary units.

(see FIG. 14W) shows a significant improvement in alignment, especially in the 450–520 nm region. As the brightness increased, the spec-

trometer was able to more accurately detect intensity variations. The match with the theoretical curve is notably better than in the previous case. Nonetheless, a dip in intensity between 550–580 nm persists and appears to be systematic. The final dataset was obtained at 22V,

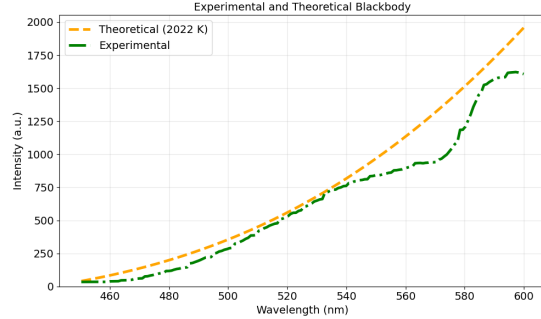


FIG. 5. Comparison of the 14V experimental spectrum and the corresponding 2022K blackbody distribution. This dataset shows the smallest deviation from theory among all measurements. “a.u.” stands for arbitrary units.

corresponding to a temperature of 2535 K (see FIG. 6). In this case, while the spectral shape follows the theoretical trend at shorter wavelengths, it deviated much at longer wavelengths. This may be due to spectral sensitivity of the camera sensor. Although the slit width was minimized (razor blades were touching physically), the intensity remained high enough to saturate the sensor and distort the measurement. This limitation likely reduced the spectrometer’s ability to distinguish intensity differences in the high-brightness regime.

All of the blackbody data are compared in FIG. 7. To show the full results, the wavelength range is extended from 400 nm to 750 nm. According to theory, there should not be a sharp peak around 600 nm, and the brightness should not drop after this point. However, in the experimental data, the curves start to fall after 600 nm. This does not match the expected blackbody shape. This was caused by the spectrometer not being sensitive enough at higher wavelengths. Even though this problem exists,

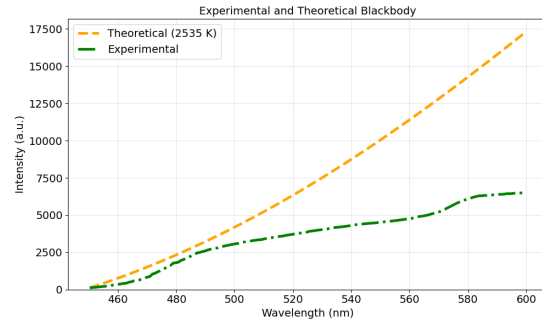


FIG. 6. Comparison of the 22V experimental spectrum and the corresponding 2535K blackbody distribution. Beyond 500 nm, the experimental curve significantly deviates from the theoretical one. “a.u.” stands for arbitrary units.

the graph still shows slight the curve shift to the left and a steeper slope between 450 nm and 600 nm as the temperature increases. This general behavior agrees with what is expected from blackbody radiation.

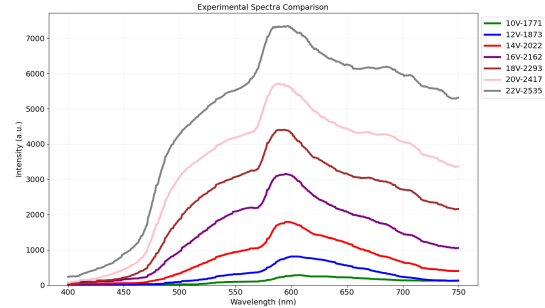


FIG. 7. Comparison of all experimental spectra. An increasing slope between 450 nm and 600 nm, along with a leftward shift of the curves as temperature increases, is observed. “a.u.” stands for arbitrary units.

Overall, the experimental results show better agreement with the theoretical blackbody curves at lower temperatures. As temperature increases, measurement accuracy decreases—likely because of detector sensitivity.

Emission Spectrum

While recording the emission spectra, the flame colors were observed using a Bunsen burner. Most wavelengths were too dim for the spectrometer to detect, but the brightest peaks were measured with high accuracy. First, the emission spectrum of lithium is shown in FIG. 8. This emission corresponds to a transition from

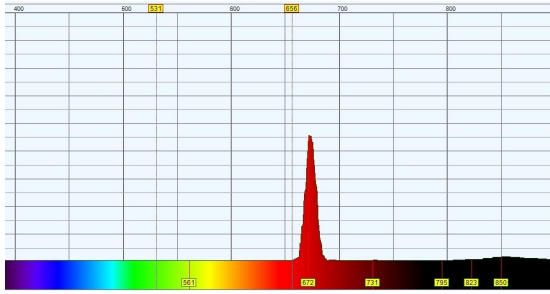


FIG. 8. Measured emission spectrum of lithium. Only the strongest peak at 672 nm is clearly visible. Expected value was 671 nm. The horizontal axis represents wavelength (nm), and the vertical axis shows intensity in arbitrary units.

the 2p to the 2s state in lithium and is expected at 671 nm. In our measurement, it appeared at 672 nm. Next, the spectrum of sodium is shown in FIG. 9. This emission corresponds to a trans-

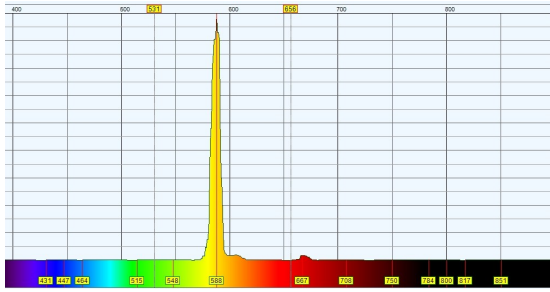


FIG. 9. Measured emission spectrum of sodium. The emission spectrum of sodium shows a single strong peak at 588 nm, close to the expected 589 nm. The horizontal axis represents wavelength (nm), and the vertical axis shows intensity in arbitrary units.

sition from the 3p to the 3s state in sodium and should appear at 589 nm. Our result showed it at 588 nm. Finally, the spectrum of potassium is shown in FIG. 10. This emission cor-



FIG. 10. Measured emission spectrum of potassium. The measured spectrum displays a dominant emission line at 773 nm, in good agreement with the expected position at 770 nm. The horizontal axis represents wavelength (nm), and the vertical axis shows intensity in arbitrary units.

responds to a transition from the 4p to the 4s state in potassium and should be at 770 nm. The spectrometer recorded it at 773 nm. Although potassium's flame color is hard to see by eye, its peak had much higher intensity than the others. This shows that the setup is able to detect near-infrared light as well as visible light.

Repeated experiments verified that the peak positions were consistent within ± 1 nm. As a result, it was observed that atomic emissions were discrete and occurred only at specific wavelengths. The agreement with the reference data confirmed the accuracy of the spectrometer.

ERROR ANALYSIS

First, the resolution of the spectrometer was limited by the quality of the webcam and the CD. From the obtained dataset, it is observed that the resolution of the spectrometer is 0.9 nm. This can be improved by using higher quality camera or placing the camera to the diffraction grating closer.

Moreover, a CD is not a perfect diffraction

grating. Its grooves form a spiral pattern starting from the center, which causes the groove alignment to become increasingly distorted as the light moves outward. If the grooves were arranged linearly, more accurate results could be obtained.

Furthermore, the diffuser used to homogenize the light limited our ability to analyze low-intensity sources. As a result, only the brightest peaks could be observed during the flame color test.

In addition, the distortion of the blackbody spectrum after 600 nm can be explained by the sensor's response. Although most cameras can detect infrared light, their sensitivity drops beyond 600 nm [9]. According to sensor data, the detection is strongest around this wavelength. After that point, the response gradually decreases. As a result, the measured blackbody spectrum shows a drop instead of the expected rise. This is not a physical effect, but a limitation of the camera used in the spectrometer.

Third, the calibration was done using green (532 ± 10 nm) and red (655 ± 10 nm) lasers. These lasers helped with general calibration, but their ± 10 nm uncertainty affected the accuracy. Later, the calibration was improved by comparing with known colors from a phone screen. This reduced the uncertainty to about ± 2 nm. However, this uncertainty can be further reduced by using laboratory-standard lasers.

Finally, the drop between 550-580 nm is not caused by the angle or the bulb itself. Because similar drops were observed when different bulbs and angles were tested. While the exact cause remains unclear, it is possible that the CD or the camera lens absorbs some of the radiation within that wavelength range.

CONCLUSION

This experiment aimed to analyze blackbody radiation and emission spectra of alkali metals using a homemade spectrometer, and to

compare the experimental results with theoretical expectations. The experimental spectra of the incandescent bulb followed Planck's blackbody distribution within the visible range, especially between 450–600 nm. The best agreement with theory was observed at 14V (2022 K). The deviation from the theoretical blackbody curve increased with temperature. However, the expected increase in slope and the shift of the curve toward shorter wavelengths were clearly observed. In addition, the atomic emission spectra obtained from the flame tests confirmed the quantized nature of atomic energy levels. The measured wavelengths showed good agreement with theoretical values (± 3 nm), indicating that the spectrometer is sufficiently accurate and precise for this experiment. A consistent dip in intensity between 550–580 nm was observed in all blackbody curves, likely due to absorptions on CD or camera lens. Deviations beyond 600 nm are attributed to the reduced infrared sensitivity of the camera sensor. Despite the limitations of the homemade spectrometer, the results support Planck's law and demonstrate the quantized nature of atomic emission. The experiment offered meaningful insight into experimental methods and the principles of quantum physics.

* berkay.buz@ug.bilkent.edu.tr

- [1] R. Harris, *Modern Physics* (Pearson Education, 2014) Chap. 2.
- [2] W. G. Schrenk, *Analytical Atomic Spectroscopy.*, Modern Analytical Chemistry (Springer US, 1975) pp. 1–10.
- [3] C. Bradley W. and O. Dale A., *An Introduction to Modern Astrophysics.* (Cambridge University Press (CUP), 2017) pp. 113–116.
- [4] P. W. Atkins, *Physical Chemistry* (W.H. Freeman and Company, 1998) pp. 251–253.
- [5] C. Kittel and H. Kroemer, *Thermal Physics* (W.H. Freeman, 1980) pp. 91–97.
- [6] J. Sansonetti and W. Martin, en *Handbook of Basic Atomic Spectroscopic Data*, 34 No 4 (Handbook of Basic Atomic Spectroscopic Data,

2005).

[7] T. Pencheva, B. Gyoch, and P. Mashkov, Optical measurements upon compact discs in education in optoelectronics (2010) pp. 531–535.

[8] H.-S. Yeo, J. Lee, A. Bianchi, D. Harris-Birtill, and A. Quigley, Specam: sensing surface color and material with the front-facing camera of a mobile device, in *Proceedings of the 19th International Conference on Human-Computer Interaction with Mobile Devices and Services*, MobileHCI '17 (Association for Computing Machinery, New York, NY, USA, 2017).

[9] Toshiba Corporation, TCD2717BFG – CCD Linear Image Sensor, <https://www.alldatasheet.com/html-pdf/1519481/TOSHIBA/TCD2717BFG/5273/15/TCD2717BFG.html> (2013), datasheet, Rev. 1.0.

APPENDIX

Python Code for Data Analysis

```

1 import pandas as pd
2 import matplotlib.pyplot as plt
3 import numpy as np
4
5 # --- Planck's Law for Blackbody Radiation ---
6 def planck(wavelength_nm, temperature_K):
7     wavelength_m = wavelength_nm * 1e-9 # nm
8     m
9     h = 6.62607015e-34 # Planck's constant (J s)
10    c = 2.99792458e8 # Speed of light (m/s)
11    k = 1.380649e-23 # Boltzmann constant (J/K)
12    numerator = 8 * np.pi * h * c
13    denominator = (wavelength_m ** 5) * (np.exp(h * c) / (wavelength_m * k * temperature_K)) - 1)
14    return numerator / denominator
15
16 # --- Load & Clean Data ---
17 file_path = r'C:\Users\hacib\OneDrive\Masaüstü\Deney212\ampul25W-14V-RGB.csv'
18 try:
19     data = pd.read_csv(file_path, sep=';|,|\t',
20                         engine='python', skiprows=18,
21                         names=['Nanometers', 'Intensity'],
22                         decimal=',')
23     data['Nanometers'] = pd.to_numeric(data['Nanometers'].astype(str).str.replace(',','.'), errors='coerce')
24     data['Intensity'] = pd.to_numeric(data['Intensity'].astype(str).str.replace(',','.'), errors='coerce')
25     data.dropna(inplace=True)
26 except Exception as e:
27     print(f"Error loading file: {e}")

```

```

25         exit()
26
27 # --- Filter Wavelength Range ---
28 data = data[(data['Nanometers'] >= 450) & (data['Nanometers'] <= 600)]
29
30 # --- Blackbody Calculation ---
31 temperature_K = 2022
32 wavelengths_nm = data['Nanometers'].values
33 bb_intensity = planck(wavelengths_nm,
34                       temperature_K)
35
36 # --- Add Blackbody to Experimental Data ---
37 exp_curve = data['Intensity'] - 110
38
39 # --- Plot All Curves ---
40 plt.figure(figsize=(10, 6))
41 plt.plot(data['Nanometers'], bb_intensity
42           *4.6-130, '--',
43           label='Theoretical ({temperature_K} K)', color='orange', linewidth=3.5)
44 plt.plot(data['Nanometers'], exp_curve, '-. ',
45           label='Experimental', color='green',
46           linewidth=3.5)
47
48 plt.xlabel('Wavelength (nm)', fontsize=14)
49 plt.ylabel('Intensity (a.u.)', fontsize=14)
50 plt.title('Experimental and Theoretical
51 Blackbody', fontsize=14)
52 plt.xticks(fontsize=14)
53 plt.yticks(fontsize=14)
54 plt.grid(True, alpha=0.3)
55 plt.legend(fontsize=14)
56 plt.ylim(bottom=0)
57 plt.tight_layout()
58 plt.show()

```

Listing 1. Python script for blackbody data analysis

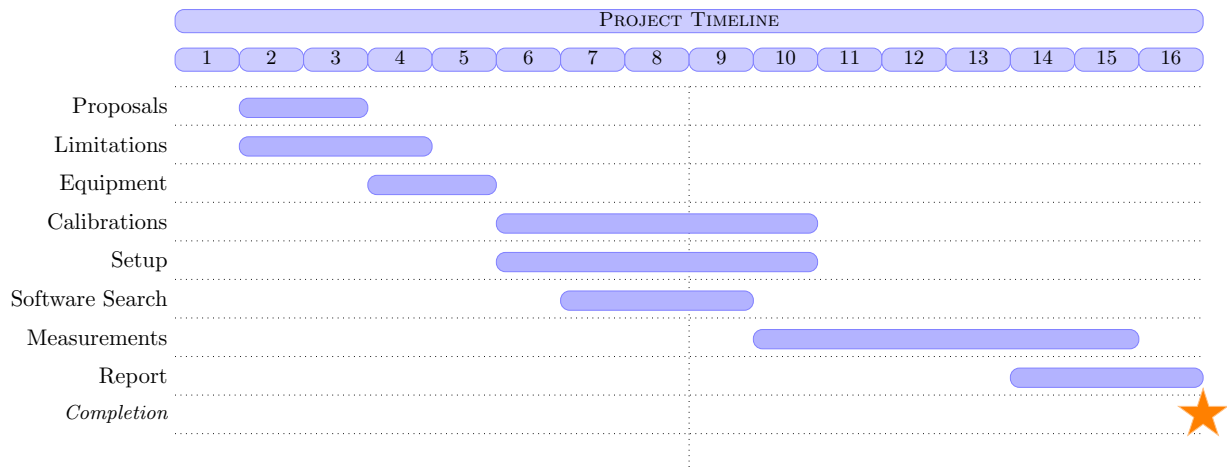
GANTT CHART

FIG. 11. Project timeline showing key milestones and activities